J|A|C|S ARTICLES

Published on Web 12/31/2009

Cyclic Tetrathiophenes Planarized by Silicon and Sulfur Bridges Bearing Antiaromatic Cyclooctatetraene Core: Syntheses, Structures, and Properties

Takeshi Ohmae, Tohru Nishinaga,* Mo Wu, and Masahiko Iyoda*

Department of Chemistry, Graduate School of Science and Engineering, Tokyo Metropolitan University, Hachioji, Tokyo 192-0397, Japan

Received September 25, 2009; E-mail: nishinaga-tohru@tmu.ac.jp; iyoda@tmu.ac.jp

Abstract: Cyclic tetrathiophenes **1**, **2**, and **3** planarized by dimethylsilyl, sulfur, and sulfone bridges bearing an antiaromatic cycloocatatetraene (COT) core were designed and synthesized to investigate the relationship among the bent angle, paratropicity, and HOMO−LUMO gap of the COT ring. The bent angles of the central COT rings of **1**−**3** were theoretically estimated and experimentally determined, and it was found that the planarity of the COT ring was finely adjusted in the order of **2** > **3** > **1** by using the small differences in the bond lengths between the bridging units and thiophene rings. From the comparisons of NICS values and calculated HOMO−LUMO gaps of cyclooctatetraene at various bent angles as well as the optimized structures of cyclic tetrathiophenes **1**−**3**, similar enhancement of the paratropicity and narrowing of the HOMO−LUMO gap with decreasing bent angle of the COT rings were shown in both cyclooctatetraene and cyclic tetrathiophenes **1**−**3**. Such predictions were experimentally proved for the first time by means of ^{1}H NMR and UV−vis measurements of **1**−**3**. In comparison of the ^{1}H NMR chemical shifts of **1**−**3** with those of the corresponding precursors, upfield shifts due to a paratropic ring current in the COT ring were observed and the degree of shift increased with increasing planarity of the COT ring. Furthermore the colors of the solutions of **1** (λ_{max} = 483 nm), **2b** (λ_{max} = 618 nm), and **3b** (λ_{max} = 575 nm) were orange, purple, and red in CH_2Cl_2, respectively, indicating that the HOMO−LUMO gaps of **1**−**3** become increasingly narrow with increasing planarity of the COT ring. Reflecting these electronic properties, CV measurements demonstrated the amphoteric redox properties of **1** and **2b**, and the radical cation **1**$^{\bullet+}$, radical anion **1**$^{\bullet-}$, and dianion **1**$^{2-}$ were chemically generated and successfully characterized by means of UV−vis, ESR, and NMR spectroscopies.

Introduction

In recent years, there has been renewed interest in planarized cyclooctatetraene (COT)[1] from both theoretical[2−4] and experimental[5−9] viewpoints. COT has an inherently nonplanar tub-shaped geometry of D_{2d} symmetry with alternating single and double bonds. The dihedral angle between vicinal double bonds is 54° in the observed structure of the parent COT[10] so that the π bonds cannot conjugate well with each other. As a result, tub-shaped COT behaves as a nonaromatic cyclic olefin rather than an antiaromatic compound.[11,12] However, when a COT ring is constrained to adopt a planar structure, considerable 8π-antiaromatic paratropicity is theoretically predicted to be generated in the ring.[3]

In experiments, there are two strategies to planarize a COT ring, that is, the annelation of either small membered rings or rigid planar π-systems to the COT skeleton, and the antiaromaticity can be detected as phenomena such as shifts in ^{1}H NMR due to a paratropic ring current, weak absorption maxima at longer wavelengths, and amphoteric redox behaviors. By the use of these structural modifications, many attempts have been made to realize a planar COT ring,[5] but complete planarization of the ring with substantial paratropicity has been rather difficult. For example, COT derivatives annelated with one small cycloalkane[5i−k] or norbornane unit[5l] have been synthesized, yet these compounds possess a tub-conformation. Even in the case of the first hydrocarbon derivative with a completely planar COT ring, that is, tetrakis(bicyclo[2.1.1]hexano)COT,[7a] the antiaromaticity is considerably reduced due to the widening of the HOMO−LUMO gap[3b] by the orbital interaction between the π-system and the highly strained C−C σ-bond in the clamping units.[7b] Similarly, the tetraphenylene completely planarized by four oxygen bridges exhibits a small antiaromatic character in the central eight-membered ring,[8b] suggesting that the paratropicity of the COT ring is weakened by the fusion of aromatic

(1) Klärner, F. -G. *Angew. Chem., Int. Ed.* **2001**, *40*, 3977.
(2) (a) Trindel, C.; Wolfskill, T. *J. Org. Chem.* **1991**, *56*, 5426. (b) Pirrung, M. C.; Krishnamurthy, N.; Nunn, D. S.; Mcphaii, A. T. *J. Am. Chem. Soc.* **1991**, *113*, 4910. (c) Wenthold, P. G.; Hrovat, D. A.; Borden, W. T.; Lineberger, W. C. *Science* **1996**, *272*, 1456. (d) Scheleyer, P. v. R.; Maerker, C.; Dransfield, A.; Jiao, H.; Hommes, N. J. R. v. E. *J. Am. Chem. Soc.* **1996**, *118*, 6317. (e) Baldridge, K. K.; Siegel, J. S. *J. Am. Chem. Soc.* **2001**, *123*, 1755. (f) Baldridge, K. K.; Siegel, J. S. *J. Am. Chem. Soc.* **2002**, *124*, 5514. (g) Stanger, A. *J. Org. Chem.* **2006**, *71*, 883. (h) Shelton, G. R.; Hrovat, D. A.; Wei, H.; Borden, W. T. *J. Am. Chem. Soc.* **2006**, *128*, 12020. (i) Zhou, X.; Hrovat, D. A.; Borden, W. T. *Org. Lett.* **2008**, *10*, 893. (j) Karadakov, P. B. *J. Phys. Chem. A* **2008**, *112*, 12707. (k) Kummli, D. S.; Lobsiger, S.; Frey, H. M.; Leutwyler, S.; Stanton, J. F. *J. Phys. Chem. A* **2008**, *112*, 9134. (l) Pierrefixe, S. C. A. H. M.; Bickelhaupt, M. *J. Phys. Chem. A* **2008**, *112*, 12816.

 10.1021/ja908161r

benzene rings. In contrast, a tetrameric porphyrin sheet having a completely planar COT ring with considerable paratropicity has recently been synthesized.[9] However, electronic properties of the π system may be characterized by peripheral porphyrin units rather than by the central COT ring.

On the other hand, oligothiophenes have attracted considerable attention for their versatility in applications in electronic devices such as organic electro-luminescent devices,[13] solar cells,[14] and field effect transistors.[15,16] In addition, thiophene rings can be easily modified with various functional groups and the derivatives are mostly stable.[17] By utilizing these advantages, cyclic oligothiophenes with an antiaromatic planar COT structure can be a unique candidate for an efficient organic semiconductor. As such a structural motif, we designed cyclic tetrathiophenes **1**−**3** having a planar COT structure, which are bridged by two dimethylsilyl groups, sulfur atoms, or sulfone groups. The degree of planarization of these cyclic tetrathiophenes can be finely adjusted by changing the bridging units. Previously, we synthesized cyclic tetrathiophene **1**, but because of the low overall yield, an efficient synthetic route was required for full characterizations of the properties derived from a planar COT structure.[18a] Recently, we have reexamined the synthesis of **1** and developed an improved preparation method.[18b] Also, we have developed efficient synthetic pathways for the sulfur analogues **2** and **3**. Here, we report the syntheses, structures, paratropicity of the COT rings, and redox properties of **1**−**3**. From these experimental and theoretical results, we have succeeded, for the first time, in proving that a small change in the planarity of a COT ring causes a substantial change in the paratropicity and HOMO−LUMO gap of the π-system.

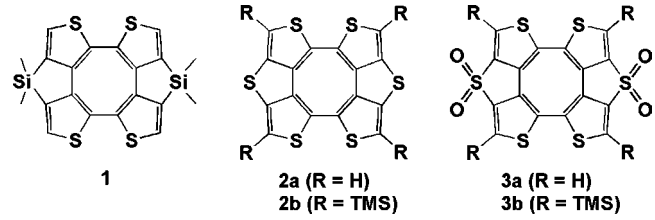

Results and Discussion

Synthesis. In our previous procedures,[18a] the synthesis of **1** was carried out using dual coupling with $CuCl_2$ of dizinc bithiophene generated from bithiophene **5** (Scheme 1).[19] The overall yield of **1** from 3,4-dibromothiophene was 2.7%. In the present study, an efficient synthetic route for **1** was developed as shown in Scheme 1. Dibromobithiophene **4**, which was prepared by the homocoupling of 3,4-dibromothiophene, was dilithiated with 2 equivalents of *n*-BuLi, and the resulting dilithiated species was treated with dichlorodimethylsilane to give **5** in 89% yield. Dilithiation of **5** with *n*-BuLi, followed by reaction with tridecafluorohexyl iodide afforded diiodide **6** in 52% yield. The selective dilithiation is probably due to the electronic effect of the silyl group. The direct lithiation of **5** with *n*-BuLi in THF, followed by treatment with $CuCl_2$ produced **1** in 33% yield. The overall yield of **1** from 3,4-dibromothiophene is 23%. In addition, the reaction of **6** with *n*-BuLi, followed by treatment with $CuCl_2$ produced **1** in 51% yield (overall 18% yield from 3,4-dibromothiophene).

Scheme 1

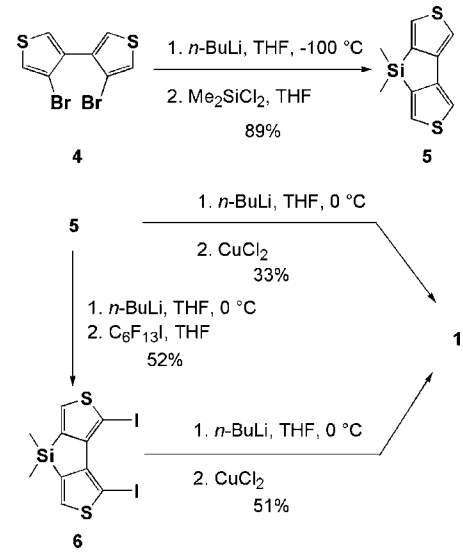

(3) (a) Fowler, P. W.; Havenith, R. W. A.; Jenneskens, L. W.; Soncini, A.; Steiner, E. *Chem. Commun.* **2001**, 2386. (b) Fowler, P. W.; Havenith, R. W. A.; Jenneskens, L. W.; Soncini, A.; Steiner, E. *Angew. Chem., Int. Ed.* **2002**, *41*, 1558. (c) Havenith, R. W. A.; Fowler, P. W.; Jenneskens, L. W. *Org. Lett.* **2006**, *8*, 1255.
(4) (a) Corminboeuf, C.; Schleyer, P. v. R.; Warner, P. *Org. Lett.* **2007**, *9*, 3263. (b) Bean, D. E.; Fowler, P. W. *Org. Lett.* **2008**, *10*, 5573. (c) Aihara, J. *J. Phys. Chem. A* **2009**, *113*, 7945.
(5) (a) Krebs, A. *Angew. Chem., Int. Ed. Engl.* **1965**, *4*, 953. (b) Seitz, G.; Pohl, L.; Pohlke, R. *Angew. Chem., Int. Ed. Engl.* **1969**, *8*, 447. (c) Wong, H. N. C.; Garrant, P. J.; Sondheimer, F. *J. Am. Chem. Soc.* **1974**, *96*, 5604. (d) Dürr, H.; Klauck, G.; Peters, K.; Schnering, H. G. V. *Angew. Chem., Int. Ed. Engl.* **1983**, *22*, 332. (e) Wilcox, C. F., Jr.; Uetrecht, J. P.; Grohman, K. K. *J. Am. Chem. Soc.* **1972**, *94*, 2532. (f) Willner, I.; Rabinovitz, M. *J. Org. Chem.* **1980**, *45*, 1628. (g) Kabuto, C.; Oda, M. *Tetrahedron Lett.* **1980**, *21*, 103. (h) Oda, M.; Oikawa, H. *Tetrahedron Lett.* **1980**, *21*, 107. (i) Elix, J. A.; Sargent, M. V.; Sondheimer, F. *J. Am. Chem. Soc.* **1967**, *89*, 180. (j) Elix, J. A.; Sargent, M. V.; Sondheimer, F. *J. Am. Chem. Soc.* **1970**, *92*, 969. (k) Paquette, L. A.; Wang, T. Z.; Cottrell, C. E. *J. Am. Chem. Soc.* **1987**, *109*, 3730–3734. (l) Klärner, F. -G.; Ehrhardt, R.; Bandmann, H.; Boese, R.; Bläser, D.; Houk, K. N.; Beno, B. R. *Chem.—Eur. J.* **1999**, *5*, 2119.
(6) (a) Soulen, R. L.; Choi, S. K.; Park, J. D. *J. Fluorine Chem.* **1973/74**, *3*, 141. (b) Einstein, F. W. B.; Willis, A. C.; Cullen, W. R.; Soulen, R. L. *J. Chem. Soc., Chem. Commun.* **1981**, 526. (c) Britton, W. E.; Ferraris, J. P.; Soulen, R. L. *J. Am. Chem. Soc.* **1982**, *104*, 5322.
(7) (a) Matsuura, A.; Komatsu, K. *J. Am. Chem. Soc.* **2001**, *123*, 1768. (b) Nishinaga, T.; Uto, T.; Inoue, R.; Matsuura, A.; Treitel, N.; Rabinoviz, M.; Komatsu, K. *Chem.—Eur. J.* **2007**, *14*, 2067.
(8) (a) Hellwinkel, D.; Reiff, G. *Angew. Chem., Int. Ed. Engl.* **1970**, *9*, 527. (b) Rathore, R.; Abdelwahed, S. H. *Tetrahedron Lett.* **2004**, *45*, 5267.
(9) (a) Nakamura, Y.; Aratani, N.; Shinokubo, H.; Takagi, A.; Kawai, T.; Matsumoto, T.; Yoon, Z. S.; Kim, D. Y.; Ahn, T. K.; Kim, D.; Muranaka, A.; Kobayashi, N.; Osuka, A. *J. Am. Chem. Soc.* **2006**, *128*, 4119. (b) Nakamura, Y.; Aratani, N.; Osuka, A. *Chem. Asian J.* **2007**, *2*, 860. (c) Nakamura, Y.; Aratani, N.; Furukawa, K.; Osuka, A. *Tetrahedron.* **2008**, *64*, 11433.
(10) (a) Traetteberg, M. *Acta Chem. Scand.* **1966**, *20*, 1724. (b) Karle, I. L. *J. Chem. Phys.* **1952**, *20*, 65.
(11) Nishinaga, T. *Sci. Synth.* **2009**, *45a*, 383.
(12) (a) Cope, A. C.; Burg, M. *J. Am. Chem. Soc.* **1952**, *74*, 168. (b) Askani, R. *Chem. Ber.* **1969**, *102*, 3304.
(13) Mishra, A.; Ma, C. Q.; Bäuerle, P. *Chem. Rev.* **2009**, *109*, 1141.
(14) Lo, S. C.; Burn, J. P. L. *Chem. Rev.* **2007**, *107*, 1097.
(15) (a) Murphy, A. R.; Frchet, J. M. *Chem. Rev.* **2007**, *107*, 1066. (b) Zaumseil, J.; Sirringhaus, H. *Chem. Rev.* **2007**, *107*, 1296.
(16) (a) Minari, T.; Miyata, Y.; Terayama, M.; Nemoto, T.; Nishinaga, T.; Komatsu, K.; Isoda, S. *Appl. Phys. Lett.* **2006**, *88*, 083514. (b) Miyata, Y.; Terayama, M.; Minari, T.; Nishinaga, T.; Nemoto, T.; Isoda, S.; Komatsu, K. *Chem. Asian J.* **2007**, *2*, 1492–1504. (c) Fujii, M.; Nishinaga, T.; Iyoda, M. *Tetrahedron Lett.* **2009**, *50*, 555.
(17) Recent examples, see: (a) Nakao, K.; Nishimura, M.; Tamachi, T.; Kuwatani, Y.; Miyasaka, H.; Nishinaga, T.; Iyoda, M. *J. Am. Chem. Soc.* **2006**, *128*, 16740. (b) Williams-Harry, M.; Bhaskar, A.; Ramakrishna, G.; Goodson, T., III; Imamura, M.; Mawatari, A.; Nakao, K.; Enozawa, H.; Nishinaga, T.; Iyoda, M. *J. Am. Chem. Soc.* **2008**, *130*, 3252. (c) Zhang, F.; Götz, G.; Winkler, H. D. F.; Schalley, C. A.; Bäuerle, P. *Angew. Chem., Int. Ed.* **2009**, *48*, 6632.

Scheme 2

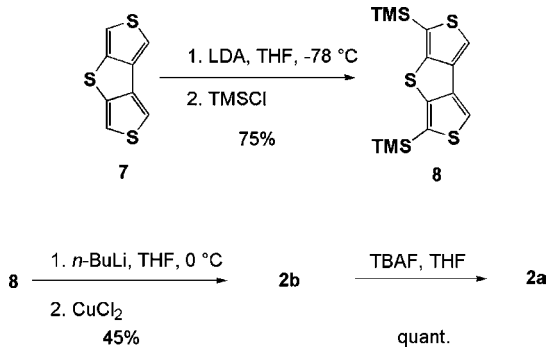

Scheme 3

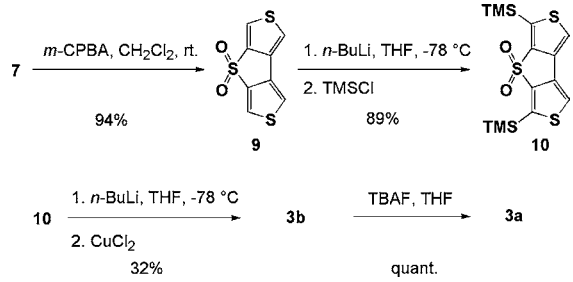

Sulfur-bridged cyclic tetrathiophene **2a** was synthesized as shown in Scheme 2. Selective dilithiation of [3,4-b:3′,4′-d]dithienothiophene (**7**)[19a] with 2 equivalents of LDA, followed by the reaction with chlorotrimethylsilane produced disilylated dithienothiophene **8**. This selective dilithiation might be attributed to the acidifying effect of the neighboring sulfur atom. Tetrasilylated sulfur-bridged cyclic tetrathiophene **2b** was synthesized in moderate yield (45%) using copper-mediated homocoupling reaction of the organolithium species derived from **8**. Deprotection reaction of **2b** with tetrabutylammonium fluoride produced the desired **2a** quantitatively.

Similarly, cyclic tetrathiophenes **3a** and **3b** were synthesized as shown in Scheme 3. Starting from sulfone **9**,[20] the selective ortholithiation of **9** with 2 equivalents of *n*-BuLi, followed by reaction with chlorotrimethylsilane yielded disilylated sulfone **10**. The selective ortholithiation is probably due to the electronic effect of the electron withdrawing sulfone unit. In a similar manner as the formation of **1** and **2b**, tetrasilylated cyclic tetrathiophene **3b** was synthesized in moderate yield (32%) using copper-mediated homocoupling reaction of organolithium species derived from **10**. Deprotection reaction of **3b** with tetrabutylammonium fluoride produced **3a** quantitatively.

Structures. Recrystallizations of **1**, **2b**, and **3b** from hexane-benzene and sublimation of **2a** gave single crystals suitable for X-ray analysis. The X-ray structures of **1**, **2a**, **2b**, and **3b** and crystal packing of **2a** are depicted in Figures 1 and 2. In the crystal packing structure of **2a**, a disorder with the occupancy ratio of approximately 85:15 was found, and only dominant structures are shown in Figure 2. The structural data from X-ray analysis are summarized in Table 1 together with the results of

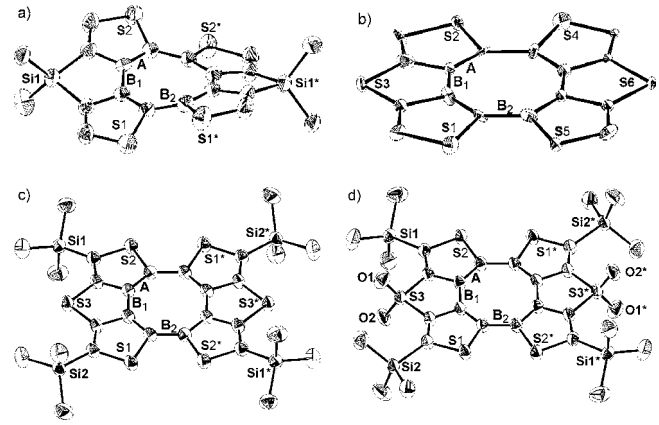

Figure 1. ORTEP drawings of X-ray structures of (a) **1**, (b) **2a**, (c) **2b**, and (d) **3b**. Thermal ellipsoids are drawn at the 50% probability level. Hydrogen atoms are omitted for clarity.

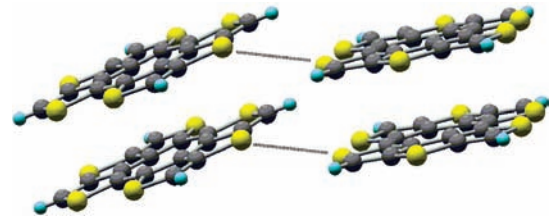

Figure 2. Packing structure of **2a**.

theoretical calculations (RB3LYP/6-31G(d,p)). As for the inner angles of the central eight-membered ring, the average values in the X-ray structures of **1**, **2a**, **2b**, and **3b** are 133.5, 135.0, 135.0, and 134.7°, respectively, which are close to the inner angle of regular octagon (135.0°). In contrast, the averaged bent angles $\alpha_{X\text{-}ray}$ of **1**, **2a**, **2b**, and **3b** determined by X-ray analysis are 18, 3.0, 3.0, and 3.2°, respectively, which are substantially smaller than the $\alpha_{X\text{-}ray}$ value (39°) of corresponding parent cyclic tetrathiophene **11**.[21] Thus, silicon, sulfur, and sulfone bridges effectively force the central COT ring to have a nearly planar structure. The significantly planar structures of **2a**, **2b**, and **3b** compared with **1** are ascribed to the C−S bonds in **2a** (1.772(4) Å), **2b** (1.758(2) Å), and **3b** (1.767(2) Å) being shorter than the C−Si bond (1.872(2) Å) in **1**. These $\alpha_{X\text{-}ray}$ values were well reproduced by the DFT calculations except for **3b**. The somewhat small $\alpha_{X\text{-}ray}$ (3.2°) for **3b** compared with the α_{calcd} (7.0°) for **3a** is probably due to the crystal packing force. In the calculated structures, the C−S bond length of **3a** (1.792 Å) is slightly longer than that of **2a** (1.770 Å), probably owing to the difference in the aromaticity of the bridging rings, that is, thiophene and thiophenedioxide. As a consequence, the α_{calcd} (4.2°) for **2a** is smaller than that for **3a** in the gas phase. These calculated results were in qualitative agreement with the observed results that the upfield shift for **2a** in DMSO solution due to a paratropic ring current of the planarized COT ring is greater than that of **3a** and that the longest absorption maximum of **2b** in CH_2Cl_2 solution is bathochromically shifted compared with that of **3b** (see below).

(18) (a) Kabir, S. M. H.; Miura, M.; Sasaki, S.; Harada, G.; Kuwatani, Y.; Yoshida, M.; Iyoda, M. *Heterocycles* **2000**, *52*, 761. (b) Iyoda, M. *Adv. Synth. Catal.* **2009**, *10*, 984.
(19) (a) Iyoda, M.; Miura, M.; Sasaki, S.; Harada, G.; Kabir, S. M. H.; Kuwatani, Y.; Yoshida, M. *Tetrahedron Lett.* **1997**, *38*, 4581. (b) Miyake, Y.; Wu, M.; Rahman, M. J.; Iyoda, M. *Chem. Commun.* **2005**, 411.
(20) Janssen, M. J.; DeJong, F. *J. Org. Chem.* **1971**, *36*, 1645.
(21) (a) Kauffmann, T.; Greving, B.; Kriegesmann, R.; Mitschker, A.; Woltermann, A. *Chem. Ber.* **1978**, *111*, 1330. (b) Kauffmann, T. *Angew. Chem., Int. Ed. Engl.* **1979**, *18*, 1. (c) Marsella, M. J.; Reid, R. J. *Macromolecules* **1999**, *32*, 5982. (d) Marsella, M. J.; Reid, R. J.; Estassi, S.; Wang, L.-S. *J. Am. Chem. Soc.* **2002**, *124*, 12507.

Table 1. Experimental[a] and Calculated[b] Average Bond Lengths (Å), Inner Angles (deg), and Bent Angle α (deg) in the COT Ring of Cyclic Tetrathiophenes **1**−**3**, Related Compounds **11**−**17**, and Parent COT with D_{2d} and D_{4h} Symmetry

	bond A (Å)		bond B[c] (Å)		average bond length in eight-membered ring (Å)		average inner angle (deg)		bent angle α (deg)	
compd	exptl	calcd	exptl	calcd	exptl	calcd	exptl	calcd	exptl	calcd
1 (D_2)	1.378 (2)	1.383	1.465 (2)	1.470	1.421 (1)	1.427	133.5	133.4	18	19
2a (D_2)	1.384 (6)	1.387	1.461 (6)	1.460	1.422 (4)	1.424	135.0	135.0	3.0	4.3
2b (D_2)	1.377 (3)	−	1.458 (3)	−	1.418 (1)	−	135.0	−	3.0	−
3a (D_2)	−	1.383	−	1.468	−	1.425	−	134.8	−	7.0
3b (D_2)	1.369 (2)	−	1.471 (2)	−	1.420 (1)	−	134.7	−	3.2	−
11 (D_2)	1.377 (2)[d]	1.383	1.464 (2)[d]	1.467	1.421 (1)[d]	1.425	127.9[d]	127.4	39[d]	40
12 (D_{4h})	−	1.413	−	1.489	−	1.451	−	135.0	−	0.0
13 (D_{4h})	−	1.396	−	1.431	−	1.414	−	135.0	−	0.0
14 (D_2)	−	1.442	−	1.482	−	1.462	−	131.7	−	27
15 (D_2)	−	1.451	−	1.465	−	1.458	−	134.2	−	14
16 (D_{4h})	−	1.437	−	1.493	−	1.465	−	135.0	−	0.0
17 (D_{8h})	1.412 (1)[e]	1.425	1.430 (4)[e]	1.425	1.421 (1)[e]	1.425	135.0[e]	135.0	0.7[e]	0.0
COT (D_{4h})	−	1.345	−	1.476	−	1.411	−	135.0	−	0.0
COT (D_{2d})	1.340 (3)[f]	1.342	1.470 (8)[f]	1.473	1.405 (4)[f]	1.408	126.1[f]	127.7	43[f]	40

[a] Determined by X-ray analysis except for parent COT which is observed by sector electron diffraction method. [b] Calculated by RB3LYP/6-31G(d,p). [c] Average of B_1 and B_2 bond lengths. [d] Reference 21c. [e] Reference 22b. [f] Reference 10a.

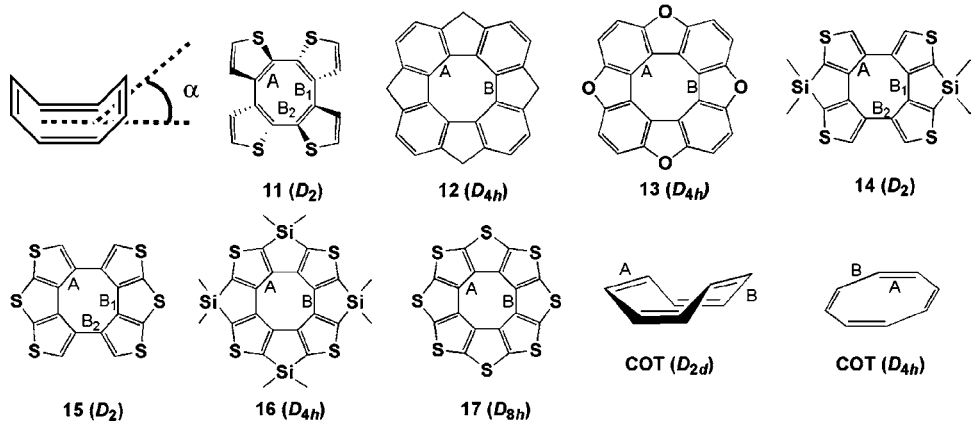

As concerns the bond lengths in the COT rings of **1**, **2a**, **2b**, and **3b** determined by X-ray analysis, the average value of bond A (see Figure 1) (A: **1**, 1.378 Å; **2a**, 1.384 Å; **2b**, 1.377 Å; **3b**, 1.369 Å) and bond B (B: **1**, 1.465 Å; **2a,** 1.461 Å; **2b**, 1.458 Å; **3b**, 1.471 Å) are almost identical to the corresponding values of their precursors **5**, **7**, and **9** obtained by X-ray analysis. The optimized structures of **1**, **2a**, and **3a** also exhibited similar bond length alternation in the COT ring (Table 1). These results indicate that the potentially unfavorable antiaromatic ring derived from the planar COT structure in **1**, **2b**, and **3b** does not affect the bond length alternation in the COT ring. To estimate the double bond character in the COT ring, the calculated average bond lengths of the central COT rings of **1**−**3** and related compounds **12**−**17**[22]were compared (Table 1). The calculated average bond lengths of tetraphenylenes **12** (1.451 Å) and **13** (1.414 Å) with the full planar COT structure are longer and shorter than those of **1**−**3** (**1**, 1.427 Å; **2a**, 1.424 Å; **3a**, 1.425 Å), respectively, while the average values of radialene type compound **14**−**17** (**14**, 1.462 Å; **15**, 1.458 Å; **16**, 1.465 Å; **17**, 1.425 Å) are longer than those of **1**−**3** except for **17**. Thus, there is no apparent relationship between the structure and the double bond character in the COT rings. Nevertheless, as described below, the cyclic tetrathiophenes **1**−**3** show the characteristic magnetic and electronic properties derived from the planarized COT ring, which is in sharp contrast to the absence of such properties for **12**−**17**.

In the packing structure of **1** (see Supporting Information), a CH-π interaction exists between the methyl proton and COT moiety, leading to a herringbone packing structure. Meanwhile, in the packing structure of **2a** (Figure 2), the molecules are aligned in a face-to-face π stacking manner and the distances between the π-planes are 3.58 Å. In addition, intercolumnar S−S interaction (3.65 Å) is present. According to recent theoretical calculations, the stacking of antiaromatic planar COT rings causes through-space aromatic stabilization.[4] However, no apparent change in bond length alternation in the COT ring was observed in **2a**, suggesting that the effect of such aromatic stabilization, if present, is negligibly small in the formation of the stacking structure of **2a**.[23]

Relationship between Paratropicity and HOMO−LUMO Gap. The NICS(0)[2d,24] and NICS(1)$_{zz}$[25] values (GIAO/HF/6-311+G(d,p)//B3LYP/6-31G(d,p)) of the COT ring and the HOMO−LUMO gaps of **1**−**3**, related compounds **11**−**17**, and parent COT with the D_{2d} and D_{4h} symmetry were calculated and the results are summarized in Table 2. In the case of the use of NICS(0) for polycyclic compounds, "double-counting" the magnetic character of separate ring system may affect the conclusions,[26] and therefore we compared the results of NICS(1)$_{zz}$ to check the potential problem.[27] The NICS(0) (and NICS(1)$_{zz}$) values of **1**, **2a**, and **3a** are 12.7 (33.3), 17.4 (44.8), and 15.4 (40.2), respectively, which are less than that of parent planar D_{4h}-COT (26.6 (62.5)) but considerably larger than that of tub-shaped D_{2d}-COT (2.9 (7.4)). For tub-shaped cyclic tetrathiophene **11,** the NICS values (3.8 (13.2)), that are almost identical to those of parent D_{2d}-COT, suggest that sulfur atoms of thiophene do not substantially affect the NICS values of the central ring, and therefore it can be concluded that the positive

Table 2. HOMO−LUMO Gap (eV)[a] of Cyclic Tetrathiophenes **1**−**3**, Related Compounds **11**−**17**, and Parent COT with D_{2d} and D_{4h} Symmetry and NICS(0) and NICS(1)$_{zz}$ (ppm)[b] of their COT Rings

compd	HOMO−LUMO gap (eV)	NICS(0) (ppm)	NICS(1)$_{zz}$ (ppm)
1 (D_2)	2.87	12.7	33.3
2a (D_2)	2.62	17.4	44.8
3a (D_2)	2.72	15.4	40.2
11 (D_2)	4.04	3.8	13.2
12 (D_{4h})	3.71	8.8	20.8
13 (D_{4h})	3.67	8.5	21.9
14 (D_2)	4.35	4.6	12.3
15 (D_2)	4.25	5.2	14.2
16 (D_{4h})	3.86	4.8	12.7
17 (D_{8h})	4.67	5.6	15.8
COT (D_{4h})	2.41	26.6	62.5
COT (D_{2d})	4.29	2.9	7.4

[a] Calculated by RB3LYP/6-31G(d,p). [b] Calculated by GIAO/HF/6-311+G(d,p)//B3LYP/6-31G(d,p).

NICS values of **1**, **2a**, and **3a** are principally due to the paratropic ring current in the central ring.

Recent theoretical studies using the "continuous transformation of origin of current density (CTOCD)" method have predicted that the paratropic ring current of planar COT is derived dominantly from HOMO−LUMO transition.[3a,b] Furthermore, the paratropic ring current was shown to survive even in a tub-shaped COT ring, when the plane to plane distance is below 0.62 Å where the planes are defined by the upper and bottom four carbons of tub-shaped COT ring.[3c] However, the relationships among the strength of paratropicity, the HOMO−LUMO gap, and the bent angle α of the COT ring have yet to be reported. Thus, we calculated the NICS values and the HOMO−LUMO gaps of cyclooctatetraene with various bent angles and the results are plotted in Figure 3. As the bent angle decreases, the NICS value of the COT ring increases (Figures 3a,b), with considerable narrowing of the HOMO−LUMO gap from 4.38 to 2.41 eV (Figure 3c).[28] Consequently, it is obvious that the strength of paratropicity is closely associated with the HOMO−LUMO gap.

As for cyclic tetrathiophenes **1**−**3**, similar enhancement of paratropicity in the central COT ring and narrowing of the HOMO−LUMO gap with increasing planarity were shown in Figure 3. In the comparison between the results of NICS(0) (Figure 3a) and NICS(1)$_{zz}$ (Figure 3b), the both NICS values for **1**−**3** are about 70−80% of those of D_{2d}-COT having similar bent angles. These results suggest that "double counting" does not have much effect on the fused COT system possibly due to the larger eight-membered ring. The smaller NICS values for

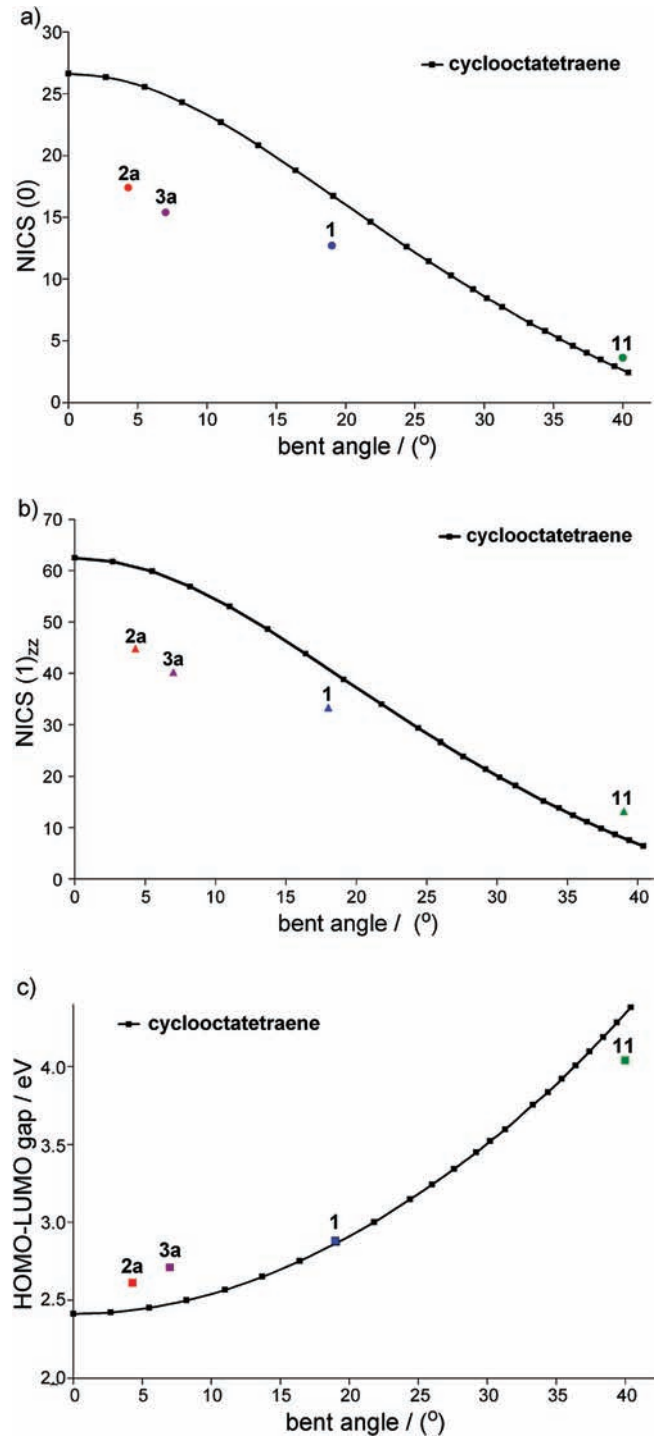

Figure 3. Correlations between (a) NICS(0) and bent angle α, (b) NICS(1)$_{zz}$ and bent angle α, and (c) HOMO−LUMO gap and bent angle α of cyclooctatetraene (black), **1** (blue), **2a** (red), **3a** (purple), and **11** (green).

1, **2a**, and **3a** compared with parent D_{4h}-COT can be ascribed principally to the larger HOMO−LUMO gaps of **1**, **2a**, and **3a**, which would be caused by the fused aromatic thiophene rings irrespective of the π-extensions. This assumption was also supported by apparently smaller NICS(0) values and larger HOMO−LUMO gap of tetraphenylene **12** (8.8 ppm and 3.71 eV) and **13** (8.5 ppm and 3.67 eV) completely planarized by four methylene and oxygen bridges. Since benzene has greater aromaticity than thiophene, the paratropic ring current of the COT ring in **12** and **13** would be reduced by benzene moieties

(22) (a) Chernichenko, K. Y.; Sumerin, V. V.; Shpanchenko, R. V.; Balenkova, E. S.; Nenajdenko, V. G. *Angew. Chem., Int. Ed.* **2006**, *45*, 7367. (b) Fujimo, T.; Suizu, R.; Yoshikawa, H.; Awaga, K. *Chem.—Eur. J.* **2008**, *14*, 6053.
(23) The NICS values (GIAO/HF/6-311+G(d,p)) of the COT ring of monomer and dimer in the X-ray structure of **2a** were similar, (16.1 and 16.5) suggesting that there is no aromatic interaction between the COT rings in the packing structure of **2a**.
(24) Chen, Z.; Wannere, C. S.; Corminboeuf, C.; Puchta, R.; Schleyer, P. v. R. *Chem. Rev.* **2005**, *105*, 3842.
(25) (a) Corminboeuf, C.; Heine, T.; Seifert, G.; Schleyer, P. v. R.; Weber, J. *Phys. Chem. Chem. Phys.* **2004**, *6*, 273–276. (b) Fallah-Bagher-Shaidaei, H.; Wannere, C. S.; Corminboeuf, C.; Puchta, R.; Schleyer, P. v. R. *Org. Lett.* **2006**, *8*, 863–866.
(26) Mills, N. S.; Llagostera, K. B. *J. Org. Chem.* **2007**, *72*, 9163.
(27) We thank a reviewer for raising this point.
(28) At the same time, the gap between the HOMO-1 and HOMO considerably increases. See: (a) Nishinaga, T.; Komatsu, K.; Sugita, N.; Lindner, H. J.; Richter, J. *J. Am. Chem. Soc.* **1993**, *115*, 11642. (b) Nishinaga, T.; Uto, T.; Komatsu, K. *Org. Lett.* **2004**, *6*, 4611.

Table 3. NICS (0) (ppm) of Thiophene Ring and Observed and Calculated ^{1}H NMR Chemical Shifts (ppm) of Thiophene Proton of **1**−**3**, **5**, **7**, and **9**

compd	NICS(0)[a] (ppm)	exptl (δ/ppm)	calcd[a] (δ/ppm)
1	−9.25	7.26	7.42
2a	−10.59	6.97	6.53
3a	−11.50	7.99	7.70
5	−11.27	7.53	7.67
7	−13.02	7.39	7.20
9	−13.49	8.29	8.26

[a] Calculated by GIAO/HF/6-311+G(d,p)// B3LYP/6-31G(d,p).

more than by thiophene moieties in **1**−**3**. On the other hand, note that the formal position of the double bonds is critical for occurrence of the paratropicity. In the cases of hypothetical planar cyclic tetrathiophenes **14** and **15**, in which the double bonds of thiophene units are located outside of the central eight-membered ring, the NICS values were shown to be 4.6 and 5.2, respectively, indicating almost no paratropic nature in the ring. Similarly, hypothetical cyclic tetrathiophene **16** and recently synthesized sulflower **17**,[22] which possess a full planar eight-membered ring, were also found to show small NICS(0) values (4.8 and 5.6, respectively). Note that the NICS values are not related with the average bond lengths in the central COT ring (see above).

^{1}H NMR. The chemical shifts of ^{1}H NMR can be a good measure for the estimation of paratropicity. Thus, we compared the changes in the chemical shifts of the α-protons of thiophene units in **1**, **2a**, and **3a** and the TMS-protons of **2b** and **3b** from the corresponding protons of their precursors **5** and **7**−**10**. Because of the low solubilities of **2a** and **3a** in common organic solvents, the ^{1}H NMR measurements were carried out in DMSO-d_6 at 120 °C for the comparison among **1**, **2a**, and **3a**, while ^{1}H NMR spectra of **2b** and **3b** as well as **11** were measured in $CDCl_3$ at room temperature. In the case of tetrathiophene **11** bearing a tub-shaped COT ring, not an upfield shift but rather a downfield shift was observed for the α-proton of thiophene in **11** (δ 7.37) in comparison with the corresponding proton of 3,3′-bithiophene (δ 7.20),[29] indicating there is no paratropic ring current in **11**. In sharp contrast, for **2a** having the highest planarity among **1**−**3**, the thiophene proton (δ 6.97) showed a 0.42 ppm upfield shift compared with the corresponding proton of **7** (δ 7.39)[29] as summarized in Table 3. Similarly, the thiophene protons of **1** and **3a** were observed at δ 7.26 and 7.99, respectively, which were also shifted upfield relative to the corresponding protons of **5** and **9** (δ 7.53, 8.29)[29] by 0.27 and 0.30 ppm, respectively, but to a smaller extent than that in **2a**. Similarly the NMR chemical shifts of TMS-protons in **2b** and **3b** (δ 0.30, 0.41) showed 0.10 and 0.09 ppm upfield shifts relative to the corresponding protons of **8** and **10** (δ 0.40, 0.50) in $CDCl_3$.

To clarify the origin of the observed upfield shifts in the thiophene protons, several factors involving changes in structural and magnetic properties upon the formation of the COT structure should be taken into consideration. However, since no apparent structural change was observed in both X-ray and calculated structures as described above, the change in magnetic properties is considered to be more important. Among the factors of magnetic properties, both generation of paratropicity of the central COT ring and decrease of diatropicity in the thiophene rings upon the formation of the COT structure are able to cause the upfield shifts. Thus, the differences of the calculated NMR chemical shifts of the thiophene protons between the cyclic tetrathiophenes and their precursors ($\Delta\delta_{calcd}$) as well as the NICS (0) values of the thiophene rings of **1**, **2a**, **3a**, **5**, **7**, and **9** were compared. As calculated from the data shown in Table 3, the degree of upfield shift of the thiophene proton (**2a**, $\Delta\delta_{calcd}$ = 7.20 − 6.53 = 0.67; **3a**, $\Delta\delta_{calcd}$ = 8.26 − 7.70 = 0.56; **1**, $\Delta\delta_{calcd}$ = 7.67 − 7.42 = 0.25) enlarges in accordance with the planarity of the COT ring, which is in qualitative agreement with the observed results. As for the change in diatropicity of the thiophene rings, the differences of the NICS(0) values between cyclic tetrathiophenes **1** (−9.25), **2a** (−10.59), **3a** (−11.50) and their precursors **5** (−11.27), **7** (−13.02), and **9** (−13.49) are 2.43 for **2a**, 1.99 for **3a**, 2.02 for **1**, respectively. Among them, there is no substantial difference in the decrease of diatropicity for **3a** and **1** judging from the change of the NICS values, whereas the upfield shift of the thiophene proton for **3a** ($\Delta\delta_{calcd}$ = 0.56) is apparently larger than that for **1** ($\Delta\delta_{calcd}$ = 0.25). These results indicate that the decrease of diatropicity of the thiophene rings is not correlated with the upfield shift of the thiophene proton, and hence it can be concluded that the upfield shifts of the thiophene protons for **1**−**3** are principally ascribed to paratropic ring current of the COT ring. Accordingly, the observed larger upfield shifts for the thiophene proton of **2a** and the TMS proton of **2b** are the experimental proofs that the paratropic ring current of the COT part in **2** is the highest among **1**−**3**. Note that the upfield shifts in **1**−**3** seem to be in qualitative agreement with the calculated structures rather than the X-ray structures in which there is no apparent difference in the bent angles between **2b** and **3b**.

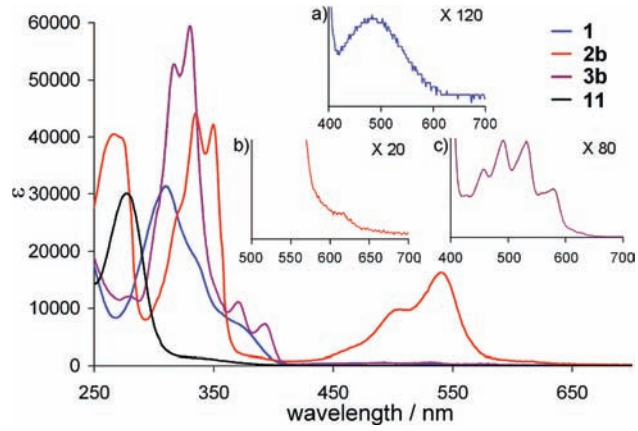

Figure 4. Absorption spectra of **1** (blue), **2b** (red), **3b** (purple), and **11** (black) in CH_2Cl_2. Insets: magnified views of (a) **1**, (b) **2b**, and (c) **3b**.

Electronic Absorption Spectra. The electronic absorption spectra of cyclic tetrathiophenes **1**, **2b**, **3b**, and **11** in CH_2Cl_2 are shown in Figure 4. The longest absorption maxima of **1**, **2b**, and **3b** in CH_2Cl_2 solutions were observed at 483, 618, and 575 nm with very weak absorption coefficients (ϵ) of 461, 801, and 355 (Table 4), and the colors of CH_2Cl_2 solutions were orange, purple, and red, respectively. The absorptions at visible regions of **1**, **2b**, and **3b** are in sharp contrast to colorless **11** (λ_{max} = 335 nm) and the weak absorption bands are quite similar to the absorption of a completely planar COT annelated with bicyclo[2.1.1]hexane units (λ_{max} = 459 nm, ϵ = 455),[7] suggesting the longest absorption bands of **1**, **2b**, and **3b** are principally ascribed to the planar COT structure. Actually, the

(29) The observed NMR chemical shifts for the α-protons of 3,3′-bithiophene, **5**, **7**, **9**, and **11** and the carbons of **1** and **12** were assigned according to the calculated NMR chemical shifts (GIAO/HF/6-311+G(2d,p)//B3LYP/6-31G(d,p) level).

Table 4. Observed and Calculated Transition Energies (nm) and Oscillator Strengths (*f*) of Cyclic Tetrathiophenes **1**, **2b**, **3b**, and **11**

	exptl		calcd[a]	
compd	λ_{max} (ϵ)	cut off (nm)	ΔE (nm)	*f*
1	483 (461)	615	579	0.0003
2b	618 (801)	710	656	0.0000
3b	575 (355)	660	620	0.0000
11	335 (1380)	420	377	0.0092

[a] Time-dependent RB3LYP/6-31G(d) calculations at the RB3LYP/6-31G(d,p) optimized geometry.

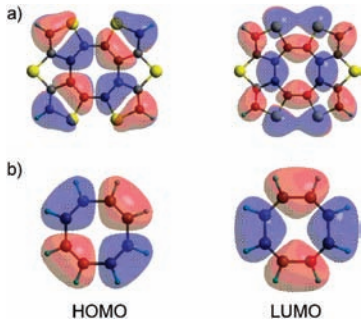

Figure 5. Kohn−Sham HOMO and LUMO of (a) **2a** and (b) COT (D_{4h}).

shape of Kohn−Sham HOMO and LUMO in the central ring of **2a** is identical with those of parent D_{4h}-COT (Figure 5). In addition, TD-DFT calculations demonstrated that the weak absorption can be assigned as a "forbidden" HOMO−LUMO transition (Table 4). Note that the coefficients of HOMO and LUMO on the bridging sulfur atoms in **2a** as well as those on the dimethylsilyl and sulfone bridges in **1** and **3a** (see Supporting Information) are negligibly small. These results indicate that the effect on the orbital interactions between the bridging units and planarized cyclic tetrathiophene moiety is negligible in the narrowing of HOMO−LUMO gaps, and hence it is considered that the planarity of the central COT ring is a dominant factor for the extraordinary long absorption maxima.[30] Such a small HOMO−LUMO gap in **2b** is quite different from that of linear quarter thiophene planarized by sulfur bridges, that is, heptathienoacene (λ_{max} = 396 nm).[31] Thus, it has been experimentally proved that a small enhancement of the planarity of the COT ring causes a surprisingly large degree of narrowing of the HOMO−LUMO gap, which is again consistent with theoretical predictions.

(30) One reviewer suggested that intramolecular charge trasfer from four thiophenes to COT core may contribute to the longer absorption bands. However, no apparent separation of charge between the thiophene and COT rings was observed in the electrostatic potential surfaces of **1**−**3** (Figure S30). Furthermore, if the fused thiophene units serve as electron-donating group to the electron-withdrawing COT core, the HOMO level of the COT core is expected to be elevated by the fused thiophene units. However, the HOMO level (−4.95 eV, B3LYP/6-31G(d,p)) of hypothetical **11** having planar D_{2h} structure was calculated to be identical to that of D_{4h}-COT (−4.95 eV). Both results suggest that the contribution of intramolecular charge transfer is less important.

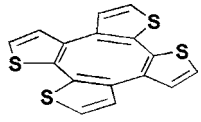

11 (D_{2h})

(31) Zhang, X.; Cote, A. P.; Matzger, A. J. *J. Am. Chem. Soc.* **2005**, *127*, 10502.

Table 5. Redox Potentials[a] (V) and HOMO and LUMO Levels[b] (eV) of Cyclic Tetrathiophenes **1**, **2b**, **3b**, and **11**

compd	$E^{ox\,c}_{1/2}$ (V)	$E^{red1\,d}_{1/2}$ (V)	$E^{red2\,d}_{1/2}$(V)	HOMO(eV)	LUMO(eV)
1	0.45	−2.09	−2.54[e]	−4.87	−2.00
2b	0.54[e]	−1.79	−2.25	−5.20	−2.59
3b	−	−1.43	−1.93	−6.08	−3.36
11	0.85[f]	−	−	−5.49	−1.45

[a] Potentials vs Fc/Fc^+. [b] Estimated by RB3LYP/6-31G(d,p). [c] Conditions, sweep rate 100 mv s^{-1}; RE: $Ag/AgNO_3$; WE: Pt wire; CE: Pt wire; solvent: CH_2Cl_2; SE: Bu_4NClO_4. [d] Conditions, sweep rate 100 mv s^{-1}; RE: $Ag/AgNO_3$; WE: glassy-carbon; CE: Pt wire; solvent: THF; SE: Bu_4NClO_4. [e] Peak potential of quasi-reversible wave. [f] Peak potential of irreversible wave.

Redox Properties. To examine the redox behaviors of cyclic tetrathiophenes **1**, **2b**, **3b**, and **11**, cyclic voltammetry was conducted at room temperature in CH_2Cl_2 for the oxidation process and in THF for the reduction process. The values of redox potentials and the Kohn−Sham HOMO and LUMO levels are summarized in Table 5. The cyclic voltammetry of **1** and **2b** exhibited not only an oxidation wave but also two step reduction waves. The reduction potentials of **2b** are lower than those of **1** because **2b** possesses a lower LUMO level partly owing to more planar COT moiety than those of **1**. Meanwhile, **3b** showed no oxidation peak due to the lower HOMO level by the electron withdrawing sulfonyl group. On the other hand, nonbridged cyclic tetrathiophene **11** exhibited only an irreversible oxidation wave at higher potentials. These observed redox potentials are in good qualitative agreement with the calculated HOMO and LUMO levels.

The chemical oxidation of **1** with $SbCl_5$ and reduction with potassium mirror were also performed to give radical cation $\mathbf{1}^{\bullet+}$, radical anion $\mathbf{1}^{\bullet-}$ and dianion $\mathbf{1}^{2-}$,[32] which are successfully characterized by UV−vis-NIR, ESR, and NMR spectra. Especially, it is noteworthy that radical cation salt $\mathbf{1}^{\bullet+}SbCl_6^-$ was isolated as an analytically pure black powder, which is in sharp contrast to the instability of $\mathbf{11}^{\bullet+}$ as observed by the irreversible oxidation wave in CV measurement. We could not carry out the chemical oxidations and reductions of **2a** and **3a** due to the solubility problem, while the generated ion radicals from **2b** and **3b** were relatively unstable probably due to the TMS groups. The electronic spectra of $\mathbf{1}^{\bullet+}$ in CH_2Cl_2 and $\mathbf{1}^{\bullet-}$ in THF are shown in Supporting Information. The solutions of $\mathbf{1}^{\bullet+}$ in CH_2Cl_2 and $\mathbf{1}^{\bullet-}$ in THF are yellow and faint green, respectively, and the longest bands extended into the NIR region owing to the open shell nature. Thus, the longest absorption maxima of $\mathbf{1}^{\bullet+}$ and $\mathbf{1}^{\bullet-}$ were observed at 1178 nm (ϵ = 5880) and 766 nm (ϵ = 737), respectively. From TD-DFT calculations, these bands were assigned as the HOMO-SOMO (999 nm, f = 0.0242) and SOMO-LUMO+1 (666 nm, f = 0.0238) transitions, respectively. Meanwhile, the THF solution of $\mathbf{1}^{2-}$ was deep purple due to strong absorption at 546 nm (ϵ = 28000). The enhanced absorption coefficients were also well reproduced by TD-DFT calculations ($\mathbf{1}^{2-}$: 540 nm, f = 0.2114).

The ESR spectra of $\mathbf{1}^{\bullet+}$ in CH_2Cl_2 (g = 2.0032) and $\mathbf{1}^{\bullet-}$ in THF (g = 2.0049) at room temperature, exhibited similar five-line signals with a binomial distribution due to the equivalent four protons in the thiophene rings as shown in Figure 6. The coupling constants were 0.260 mT for $\mathbf{1}^{\bullet+}$ and 0.166 mT for $\mathbf{1}^{\bullet-}$. The larger coupling constant of $\mathbf{1}^{\bullet+}$ as compared with that

(32) For cyclooctatetraenyl anions, see:(a) Katz, T. J.; Reinmuth, W. H.; Smith, D. E. *J. Am. Chem. Soc.* **1962**, *84*, 802. (b) Strauss, H. L.; Katz, T. J.; Fraenkel, G. K. *J. Am. Chem. Soc.* **1963**, *85*, 2360.

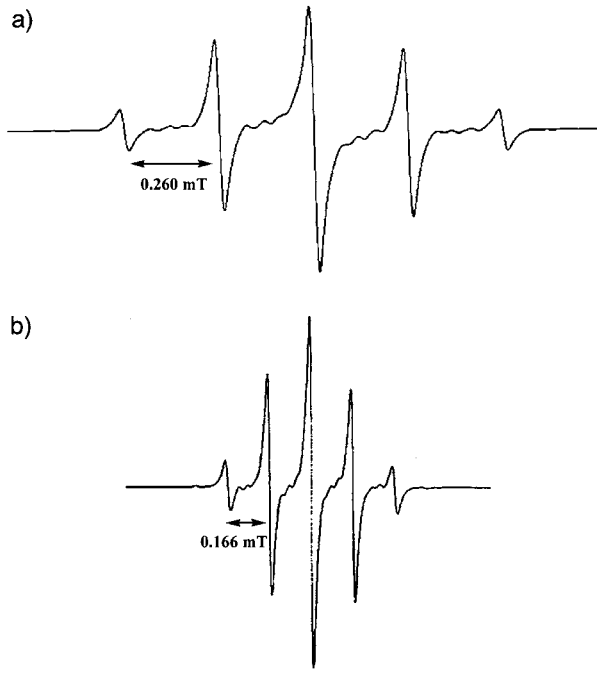

Figure 6. ESR spectra of (a) $\mathbf{1}^{\bullet+}$ and (b) $\mathbf{1}^{\bullet-}$.

of $\mathbf{1}^{\bullet-}$ is brought about by the difference between the MO coefficients on the carbon atoms connected to the protons in the HOMO and LUMO of **1**.

Next, we conducted NMR observation of $\mathbf{1}^{2-}$ in THF-d_8 at room temperature. In the NMR spectra of $\mathbf{1}^{2-}$ (Figure 7), the signals of α-protons and three out of four carbons in the thiophene ring showed upfield shifts of 0.64 ppm for the proton and 20−36 ppm for the carbons compared with those of **1**. These upfield shifts were ascribed to the shielding effects derived from the increase in electron density upon the dianion formation. Especially, in the ^{13}C NMR spectra (Figure 7b),[29] the signals of two carbons in the eight-membered ring largely shifted upfield, suggesting that the electron density tend to localize in the eight-membered ring due to the change from 8π to 10π electron systems. Actually, the electrostatic potential of $\mathbf{1}^{2-}$ computed by DFT calculations revealed a higher electron density localized in the COT ring (see Supporting Information). In contrast, methyl protons of $\mathbf{1}^{2-}$ shifted downfield by 0.08 ppm compared with those of **1** despite of the increase in the electron density of the π-system, indicating that the magnetic properties of the eight-membered ring in $\mathbf{1}^{2-}$ were changed to have an aromatic diatropicity. Judging from the NICS values of the COT rings in **1** (12.7) and $\mathbf{1}^{2-}$ (−15.8), the explanation is correct, and the central ring has a character of 10π aromatic COT dianion.

Conclusion

We have designed and synthesized novel cyclic tetrathiophenes **1**−**3** bearing a planar COT core, in which the planarity of the COT ring can be finely adjusted by using the small difference in the bond lengths between the thiophene ring and bridging atom. By virtue of the structural features, we have experimentally demonstrated for the first time that a small enhancement of planarity of the COT ring causes a considerable enhancement of the antiaromaticity and hence narrowing of the HOMO−LUMO gap as predicted by theoretical studies.[3] As a result, the oligothiophenes **1**−**3** are endowed with amphoteric redox properties, and among them,

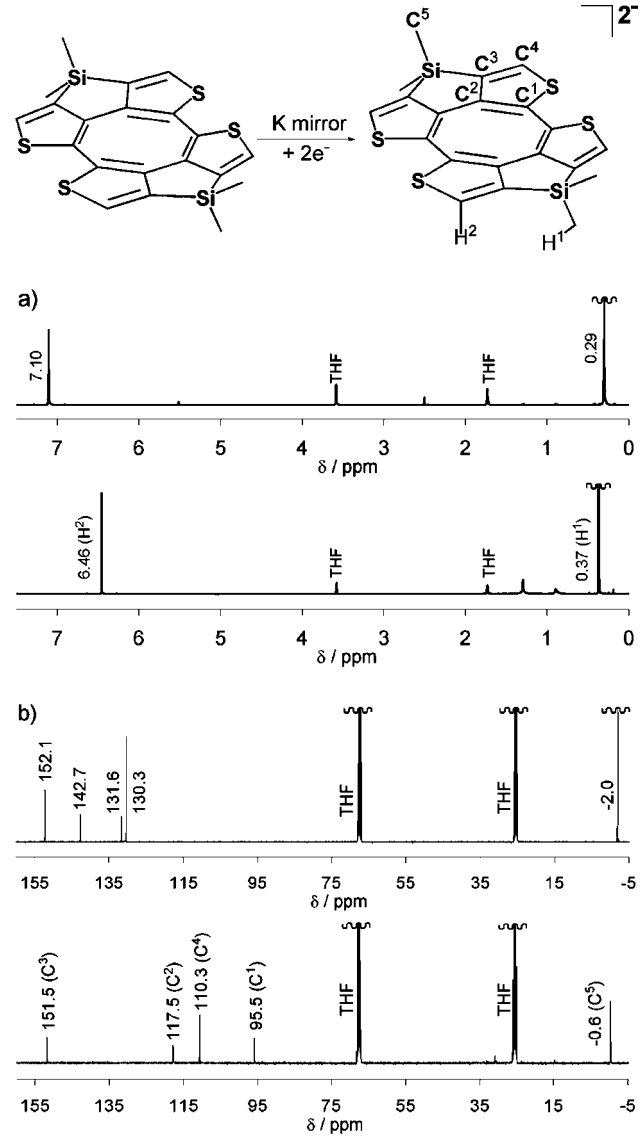

Figure 7. (a) ^{1}H (500 MHz) and (b) ^{13}C (125 MHz) NMR spectra of **1** (upper) and $\mathbf{1}^{2-}$ (lower) in THF-d_8 at room temperature.

radical cation, radical anion, and dianion of **1** were successfully characterized by means of UV−vis-NIR, ESR, and NMR spectra. Among these cyclic tetrathiophenes, a planar COT structure in **2a** was attained without bulky substituents unlike the other planar COT prepared thus far,[6,7,9] and X-ray crystallography showed a stacking structure. Thus, the structure of **2a** may be utilized as an intermolecular antiaromatic-antiaromatic interaction[3] by controlling the stacking manner with additional substituents at the side positions. Such experiments may also lead to these compounds becoming unique candidates for an efficient organic semiconductor. Experiments along this line are now underway.

Acknowledgment. This work was supported by Grant-in-Aid for Scientific Research on Priority Areas (No. 20036042, Synergy of Elements) from the Ministry of Education, Culture, Sports, Science, and Technology of Japan. We would like to thank Prof. K. Kikuchi (Tokyo Metropolitan University), Prof. W. Fujita (Tokyo Metropolitan University), and Mr. K. Sasamori (Tokyo Metropolitan University) for their assistance with low-temperature X-ray crystallography. We also thank Dr. H. Enozawa (Riken), Dr. M. Hasegawa

(Kitasato University), and Dr. M. Takase (Tokyo Metropolitan University) for helpful discussions.

Supporting Information Available: Experimental procedure and characterization data of **1**−**10**; ^{1}H and ^{13}C NMR spectra of **1**−**10**; cyclic voltammograms of **1**, **2b**, and **3b**; crystallographic data of **1**−**3b**, **5**, **7**, and **9**; absorption spectra of $\mathbf{1}^{\bullet+}$, $\mathbf{1}^{\bullet-}$, and $\mathbf{1}^{2-}$; Cartesian coordinates and total energies of the optimized structures of all calculated molecules (B3LYP/6-31G(d,p)); crystallographic information files (CIF) for **1**−**3**, **5**, **7**, and **9**. This material is available free of charge via the Internet at http://pubs.acs.org.

JA908161R